Integrating tractography in pelvic surgery: a proof of concept

Cécile Olivia Muller, Eva Mille, Alessio Virzi, Jean-Baptiste Marret, Quoc Peyrot, Alessandro Delmonte, Laureline Berteloot, Pietro Gori, Thomas Blanc, David Grévent, et al.

Ultrasound image processing to estimate the structural and functional properties of mouse skeletal muscle

Redouane Ternifi[1], Malek Kammoun[1], Philippe Pouletaut[1], Malayannan Subramaniam[2], John R. Hawse[2], and Sabine F. Bensamoun[1,*]

[1]Sorbonne Universités, Université de Technologie de Compiègne, Biomechanics and Bioengineering Laboratory, UMR CNRS 7338, Compiègne, France

[2]Department of Biochemistry and Molecular Biology, Mayo Clinic, Rochester, MN USA

[*]Correspondence and requests for materials should be addressed to S.F.B. (email: sabine.bensamoun@utc.fr)

Université de Technologie de Compiègne (UTC)

Laboratoire Biomécanique et Bioingénierie - UMR CNRS 7338

Rue Roger Couttolenc

60203 Compiègne

France

Tel: (33) 03 44 23 43 90

ABSTRACT

Noninvasive imaging techniques are increasingly used for monitoring muscle behavior in mice. However, muscle is a complex tissue that exhibits different properties under passive and active conditions. In addition to structural properties, it is also important to analyze functional characteristics. At present, such information can be obtained with ultrasound elastography. However, this technique is poorly used for small rodent models (mice and gerbils). Thus, this study aims at establish referent hindlimb muscle data, and experimental guidelines, for wild-type (WT) control mice as well as the TIEG1 knockout (KO) mouse model that is known to exhibit skeletal muscle defects.

Ultrasound was performed with the Aixplorer machine using a SLH 20-6 linear transducer probe (2.8 cm footprint). A region of interest (ROI) was placed around a superficial group of muscles. Subsequently, from the B-mode image, a classification of all the muscles and ultrasound biomarkers such as echo intensity and texture anisotropy have been determined. The influence of the gain setting (from 40% to 70%) was analyzed on these parameters. Moreover, the elasticity (E) was also measured within the ROI.

This study provides a suitable methodology for collecting experimental data: 1) the correct range of gain (between 50% and 70%) to apply for the ultrasound measurement of muscle structure, 2) the structural and functional referent data for a group of healthy muscles, 3) the gray scale index, the texture anisotropy and the elasticity (E_{TIEG1_KO}=36.1 ± 10.3kPa, E_{WT}=44.4 ± 13.4kPa) parameters, which were obtained for a group of muscles as a function of genotype.

1. Introduction

The functional properties of animal muscle can be characterized *in vitro* using mechanical tests (stretch, relaxation, indentation, etc…) to measure their passive and active mechanical properties [1] or *in vivo* using non-invasive techniques such as imaging devices or surface electromyography [2] to elucidate their physiological activity. Magnetic Resonance Imaging (MRI) has been extensively performed on rodent muscle to analyze the physiological composition (percentage of fat and water, presence of fibrosis, texture…) and muscle metabolism (creatine, choline, lipid …) through spectroscopy acquisitions. MRI can also reveal the anisotropic muscle behavior using a diffusion tensor imaging sequence. While MRI offers extensive information about the muscle structural properties, the quantification of the functional properties relating to elasticity cannot be determined by this imaging technique.

More recently, quantitative muscle ultrasound shear wave elastography (SWE), performed with the Aixplorer machine, has been reported to be an effective technique for the non-invasive assessment of the functional properties of human skeletal muscle [3,4]. Additionally, another group has used the Aixplorer machine to examine the correlation between the elastic properties and pathological characteristics of spinal cord injuries in a rat model [5]. However, in the literature, there is an important lack of studies using elastography techniques on small rodents (such as mice and gerbils). Recently, we have developed an SWE experimental protocol to characterize the *in vivo* elastic properties of the musculotendinous system of healthy mice. In order to further develop the use of the Aixplorer machine for these purposes, it is also necessary to establish referent data with regard to structural properties and echogenicity of muscle. For that, we analyzed the influence of the setting parameter (different gains) on ultrasound biomarkers (echo intensity, texture anisotropy) which were determined for both healthy and dystrophic mouse hindlimb muscle.

2. Materials and methods

2.1. Mice and Study design

Eight wild-type (WT) and eight TIEG1 (TGFβ Inducible Early Gene-1) knockout (KO) mice were used. The generation of TIEG1 KO mice has been previously described [6] and this model has been chosen for its known morphological (hypertrophy, muscle disorganization, …) changes and functional defects (lower elasticity, etc…) in hindlimb muscle compared to WT littermates [1,7,8]. All mice were maintained in a temperature controlled room (22 ± 2°C) with light/dark cycle of 12 hours. Animals had free access to water and were fed with standard laboratory chow ad libitum. This study was carried out in strict accordance with the recommendations in the Guide for the Care and Use of Laboratory Animals of the National Institutes of Health (Permit Number: DUO-4776).

2.2. Shear Wave Elastography (SWE) imaging

All mice were anesthetized with 1.5% isoflurane and a mixture of O_2/air (1:1) at an output of 0.7 L/min and placed in a supine position.

Landmarks were defined to place the mice and the paw in a reproducible manner. Muscles in the right hindlimb were imaged by the same operator with an ultrasound (US) machine (Aixplorer Multiwave™ System, Supersonic Imagine, Aix-en-Provence, France) using a novel SLH 20-6 linear transducer probe (2.38 cm footprint, 192 composite elements, effective bandwidth from 6 to 20 MHz) (Fig. 1A).

The probe was placed on the surface of the hindlimb, which was shaved, parallel to the Achilles tendon and aligned with respect to muscle fiber orientation. To obtain ideal acoustic impedance a thin layer of acoustic gel was applied. To ensure that the probe was reproducibly placed, a visual control was performed on the B-mode (anatomical) image (Fig. 1B) where the heel and the bones (fibula and tibia) surrounded by the group of muscles are present in each ultrasound (US) acquisition for all mice.

To identify the muscles present in the B mode image, an acupuncture needle (0.25 x 25mm) was inserted within the superficial hindlimb muscles (Fig. 1B). Subsequently, a dissection of the seven muscles (Fig. 1C) was performed to allow for the superimposition of the names of the muscles with the corresponding B-mode image.

The Aixplorer Multiwave^{TM} System generates two types of waves that propagate within the tissue: a compression wave that creates a high-quality B-mode image showing the anatomical structure within the hindlimb (skin, muscle, tendon, bone), and a shear wave that provides a quantitative color-coded map (rectangular box : 1 cm x 1.5 cm) of tissue elasticity (Fig. 1D). To obtain mapping of elasticity with the shear wave elastography (SWE) sequence, the setting parameters were: musculoskeletal preset, resolution mode enabled, tissue tuner at 1540 m/s, pulse duration: 600 µs, dynamic range at 60 dB, and lateral / vertical resolution of 140 µm / 205 µm. The depth setting was fixed at 2 cm for all mice during examination to display the entire muscle. The focus range was set between 0.5 cm and 1 cm depth for all mice. The setting parameters for the B-mode were: musculoskeletal preset, pulse repetition frequency: 20 kHz, spatial resolution: 38 µm, super compound disabled, harmonic disabled penetration and HD mode. The gain can be increased or decreased as a function of the depth of the explored area. Thus, to analyze the influence of these parameters on the structural properties, four different gains (40%, 50%, 60% and 70%) were tested. Time-gain compensation was maintained in the same position for all depths.

The SWE mode is based on the generation of localized acoustic radiation force by the probe which generates a propagation of transversal waves. Assuming that the ZM muscle was linearly elastic, isotropic, homogeneous and incompressible, the range of elasticity (Young's modulus : E) was set between 0 kPa and 180 kPa, which corresponds to a shear wave velocity (V) range of 0 - 7.7 m/s using the equation $E = 3 \rho V^2$ where ρ is the density of muscle (1000 kg/m^3) [10].

130 **2.3.** Image analysis

131 In the B-mode image, the muscle group in the mouse hindlimb was visualized and a region of
132 interest (ROI) was manually drawn around the muscle tissue composed of three specific muscles
133 (Gas (#5): gastrocnemius, PB (#6): peroneus brevis and Sol (#7): soleus). To quantify structural and
134 SWE parameters, a semiautomatic method was developed using ImageJ 1.46/Java 8 software
135 (National Institute of Health, Bethesda, MD, United States) [9]. Subsequently, the ROI was
136 superimposed to the elasticity image (Fig. 1D) and by using the ROI Manager Tool of ImageJ the
137 following parameters were measured: mean, standard deviation (SD) and coefficient of variation
138 (i.e ratio of standard deviation to mean) for echo intensity (EI) and mean elasticity (E: Young's
139 modulus) parameters (Fig. 2). From the mean of echo intensity, which the gray value varies from 0
140 to 255, a gray-scale index (GSI) was defined as:

141 $$\mathrm{GSI} = 1 - \frac{1}{255\,.\,\mathrm{N}} \sum_{i=1}^{N} \mathrm{EI}_i$$

142 with EI_i the echo intensity of pixel i in the selected area [10]. When GSI is close to 1 or in contrary
143 close to 0, the B-mode image changes from dark to clear, respectively.

144 The ROI of B-mode images was also analyzed for texture analysis by computing the gradient of the
145 image and the local covariance matrix *C* using ImageJ [9]. The 2x2 covariance matrix C was
146 computed for each pixel and evaluated from local intensity variations around each pixel in a box of
147 5x5 pixels. The two eigenvalues λ of *C* were retrieved and sorted with $\lambda_1 > \lambda_2$. A texture anisotropy
148 index (TAI) was computed for each ROI and defined as the mean value of the texture image $\alpha = 1 -$
149 λ_2 / λ_1. Therefore, a TAI value close to 1 indicates the strong predominance of one orientation in the
150 ROI (i.e., strong local texture anisotropy) whereas TAI close to 0 indicates a diffuse image with no
151 predominant orientation (i.e., weak local texture anisotropy).

152

153

154

2.4. Statistical analysis

The XLSTAT^{TM} software package was used to perform all statistical analyses. All parameters were expressed as the mean ± standard deviation. Nonparametric two-sample Kolmogorov-Smirnov tests were performed in order to compare the elasticity values (E) and the B-mode values (GSI, TAI) between WT and TIEG1 KO mice. The statistical analysis was considered significant for $p < 0.05$.

3. Results and discussion

3.1. Identification of hindlimb muscle

Ultrasound acquisition, as opposed to MRI imaging, did not allow for individual visualization of all of the hindlimb muscles of mice. In the present study, the ultrasound B-mode image revealed three distinct groups of muscles (Group 1 composed of gastrocnemius (#5), peroneus brevis (#6) and soleus (#7) ; Group 2 composed of plantaris (#3) and peroneus longus (#4) and Group 3 composed of the tibialis anterior (#1) and extensor digitorum longus (#2)). Noninvasive imaging techniques are increasingly used for monitoring muscle behavior of mice. Thus, the present classification, which is quite rare in the literature, could allow for the use of an optimal ultrasound methodology to build a large database of muscle structure and function before or after a given treatment or intervention. In addition, this protocol will enable the development of a very precise automated method for the follow-up of target muscles composed specifically of slow twitch fibers such as the soleus or fast twitch fibers such as the EDL.

3.2. Influence of gain settings on echogenicity and texture anisotropy

To accurately establish the ultrasound protocol applied to hindlimb mouse muscle, the influence of gain settings on echo intensity (EI) and GSI index was analyzed.

Table 1 shows the results of the EI, GSI and TAI values. The WT and TIEG1 KO GSI varied from 0.62/0.65 to 0.36, respectively. These results provide referent GSI data as a function of the gain for

182 healthy (WT) muscle and dystrophic TIEG1 KO muscle (Fig. 3A-B). It can be noted that no
183 significant difference of GSI was measured between the two genotypes (Fig. 3C). This indicates
184 that the GSI parameter is not pertinent on US images to discriminate the two genotypes; another
185 imaging technique like MRI may be more suitable [8].
186 In WT mice, the results of the coefficient of variation (CoV) of EI as a function of the gain (G)
187 settings showed a higher mean (44.1) for the gain applied at 40% compared to the other ones (from
188 50% to 70%) (CoV between 11% and 20%). The same measurements were performed on the
189 TIEG1 KO muscle and a slightly higher range of CoV (between 14.1% to 52.8%) was found
190 compared to healthy (WT) muscle. This result demonstrated a less stable EI for dystrophic muscle.
191 It can be concluded that a gain between 50% and 70% could be used to accurately measure the EI of
192 healthy and pathological mouse muscle.
193 The TAI values remained stable as a function of the gain (Fig. 3 A-B) and were in the same
194 range (approximately 0.69) for both genotypes. This result reveals a main direction present within
195 the skeletal muscle which is a result of the fiber orientation. However, no significant TAI difference
196 was found between WT and TIEG1 KO muscle (Fig. 3 D). This result was previously confirmed
197 with MRI diffusion sequence (3 directions).
198
199 3.3 Functional properties of mouse hindlimb muscle
200 From the elastography images, no significant difference in mean stiffness or co-efficient of
201 variation was found. In particular, no significant difference in the stiffness was detected between
202 TIEG1 KO (36.1 ± 10.3 kPa) and WT (44.4 ± 13.4 kPa) muscle.
203 This is probably a limitation of the SWE technique applied to small mouse muscles, which analyzes
204 a group of muscles (gastrocnemius, peroneus brevis, soleus) having different physiological
205 behaviors, leading to a global elastic value while individual muscles could have been affected by
206 the lack of TIEG1 expression [11]. It can be noted that WT values are in the same range of values
207 found by Qin et al. (2014) for hindlimb mouse muscle using a MR elastography protocol.

4. Conclusion

This study put some light in construction and release of new experimental databases using a clinical SWE ultrasound device for the characterization of the structural and functional properties of mouse hindlimb muscle. The present study has provided an accurate ultrasound identification of the different muscles located within the hindlimb. The major goal was to realize an exploratory analysis of the collected data representing by: 1) the correct range of gain to apply for the ultrasound measurement of muscle structure, 2) the structural and functional referent data for a group of healthy mouse muscles, 3) the gray scale index, the texture anisotropy and the elasticity parameters. Future studies using phantoms with parameters and geometry similar to mouse muscle could help further the development and utilization of SWE technique for monitoring changes in skeletal muscle in small animal models, over time and in response to treatment.

Ethical statement

The protocol was approved by the French ministry of higher education, research and innovation (Permit Number: DUO-4776) and the Mayo Clinic Institutional Animal Care and Use Committee (Permit Number: A9615).

Conflict of interests

The authors declare no conflict of interests.

Acknowledgment

This work was carried out in the framework of the Labex MS2T, which was funded by the French Government, through the program ” Investments for the future” managed by the National Agency for Research (Reference ANR-11-IDEX-0004-02)

References:

[1] M. Kammoun, P. Pouletaut, F. Canon, M. Subramaniam, J.R. Hawse, M. Vayssade, S.F. Bensamoun, Impact of TIEG1 deletion on the passive mechanical properties of fast and slow twitch skeletal muscles in female mice, PLoS One. 11 (2016) 1–15.

[2] K.F. Szűcs, G. Grosz, M. Süle, A. Sztojkov-Ivanov, E. Ducza, A. Márki, A. Kothencz, L. Balogh, R. Gáspár, Detection of stress and the effects of central nervous system depressants by gastrointestinal smooth muscle electromyography in wakeful rats, Life Sci. 205 (2018) 1–8.

[3] F. Hug, K. Tucker, J.L. Gennisson, M. Tanter, A. Nordez, Elastography for Muscle Biomechanics: Toward the Estimation of Individual Muscle Force, Exerc. Sport Sci. Rev. 43 (2015) 125–133.

[4] D. Bachasson, G.J.R. Dubois, Y. Allenbach, O. Benveniste, J.Y. Hogrel, Muscle Shear Wave Elastography in Inclusion Body Myositis: Feasibility, Reliability and Relationships with Muscle Impairments, Ultrasound Med. Biol. 44 (2018) 1423–1432.

[5] L. Jiang, Y.J. Wang, Q.Y. Wang, Q. Wang, X.M. Wei, N. Li, W.P. Guo, Z.L. Dou, Correlation between Pathological Characteristics and Young's Modulus Value of Spastic Gastrocnemius in a Spinal Cord Injury Rat Model, Biomed Res. Int. 2017 (2017).

[6] M. Subramaniam, G. Gorny, S.A. Johnsen, D.G. Monroe, G.L. Evans, D.G. Fraser, D.J. Rickard, K. Rasmussen, J.M.A. Van Deursen, R.T. Turner, M.J. Oursler, T.C. Spelsberg, TIEG1 Null Mouse-Derived Osteoblasts Are Defective in Mineralization and in Support of Osteoclast Differentiation In Vitro, Mol. Cell. Biol. 25 (2005) 1191–1199.

[7] M. Subramaniam, S. a Harris, M.J. Oursler, K. Rasmussen, B.L. Riggs, T.C. Spelsberg, Identification of a novel TGF-β-regulated gene encoding a putative zinc finger protein in human osteoblasts, Nucleic Acids Res. 23 (1995) 4907–4912.

[8] M. Kammoun, S. Meme, W. Meme, M. Subramaniam, J.R. Hawse, F. Canon, S.F. Bensamoun, Impact of TIEG1 on the structural properties of fast- and slow-twitch skeletal muscle, Muscle Nerve. 55 (2017) 410–416.

[9] C.A. Schneider, W.S. Rasband, K.W. Eliceiri, NIH Image to ImageJ: 25 years of image analysis, Nat. Methods. 9 (2012) 671–675.

[10] G.J.R. Dubois, D. Bachasson, L. Lacourpaille, O. Benveniste, J.Y. Hogrel, Local Texture Anisotropy as an Estimate of Muscle Quality in Ultrasound Imaging, Ultrasound Med. Biol. 44 (2018) 1133–1140.

[11] M. Kammoun, R. Ternifi, V. Dupres, P. Pouletaut, S. Même, W. Même, F. Szeremeta, J. Landoulsi, J.-M. Constans, F. Lafont, M. Subramaniam, J.R. Hawse, S.F. Bensamoun, Development of a novel multiphysical approach for the characterization of mechanical properties of musculotendinous tissues, Sci. Rep. 9 (2019) 7733.

FIGURES:

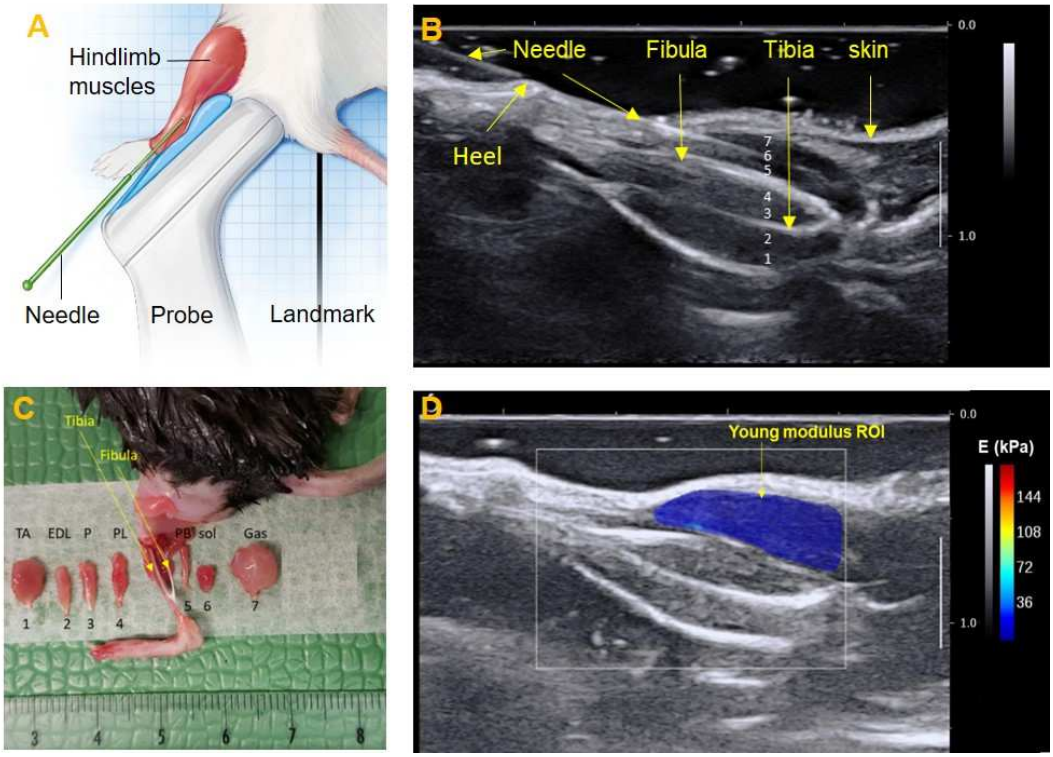

Fig. 1. (A) Ultrasound set up, **(B)** B-mode image of mice hindlimb with muscle identification using an acupuncture needle inserted in soleus. **(C)** Corresponding muscles (labeled from #1 to #7) identified on the B mode image. TA(#1): tibialis anterior, EDL(#2): extensor digitorum longus, P(#3): plantaris, PL(#4): peroneus longus, Gas(#5): gastrocnemius, PB(#6): peroneus brevis, Sol(#7): soleus. **(D)** Cartography of elasticity (E: Young modulus) with a ROI composed of 3 muscles (#5, #6, #7).

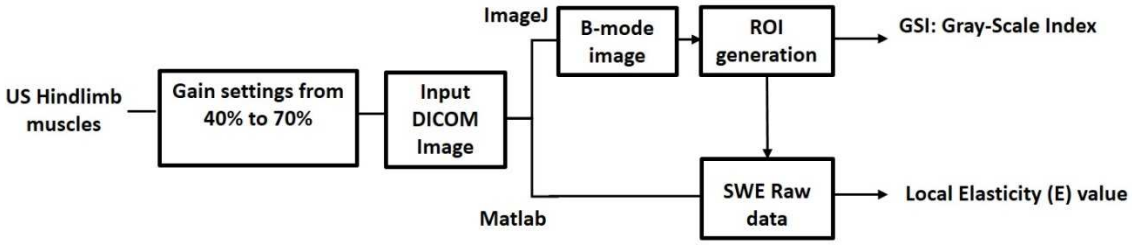

Fig. 2. Flow chart of the proposed image processing. SWE: shear wave elastography. ROI: region of interest.

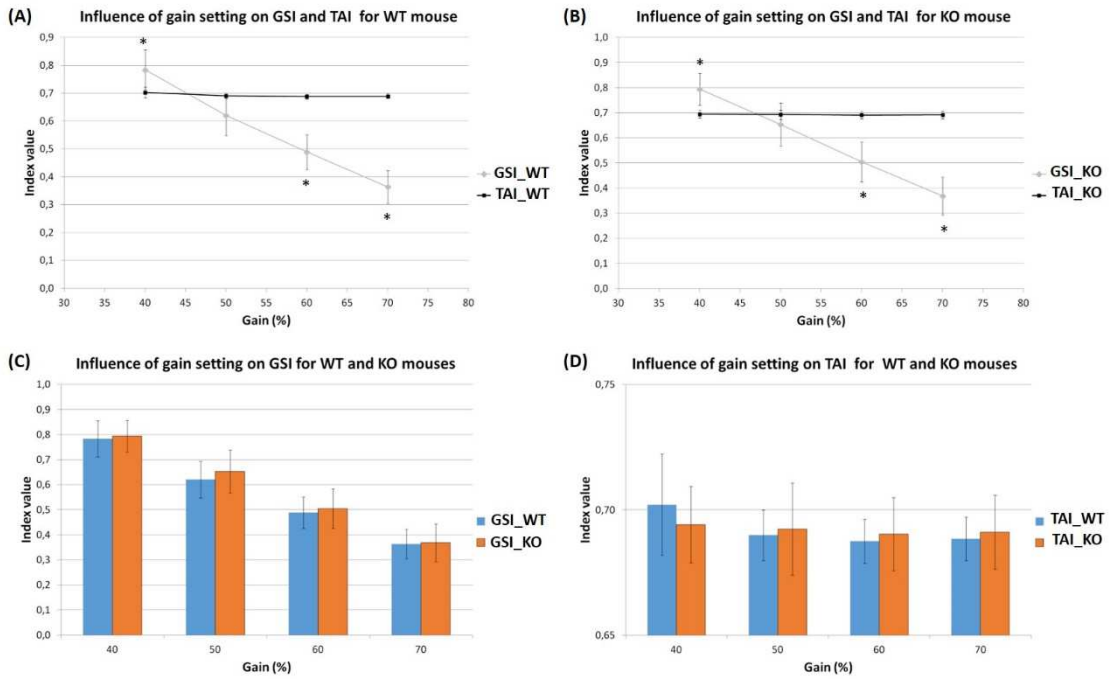

Fig. 3. Influence of gain setting on gray-scale index (GSI) and texture anisotropy index (TAI)in muscle of WT mouse (A) and KO mouse (B); Influence of gain setting on GSI (C) and on TAI (D) for both type of mouse. *Significantly different from 50% gain. Vertical bars denote standard deviation.

TABLES:

Table 1. Means results of of muscle echo intensity EI, GSI and TAI for two types of muscle (WT and TIEG1 KO).

Gain (%)	Mouse type		EI	CoV_EI (%)	GSI	TAI
40	WT (n=8)	Mean	55.3	44.1	0.783	0.702
		SD	18.4	10.0	0.072	0.020
	KO (n=8)	Mean	52.6	52.8	0.794	0.694
		SD	16.2	22.1	0.063	0.015
50	WT (n=8)	Mean	97.0	19.9	0.620	0.690
		SD	18.7	6.3	0.073	0.010
	KO (n=8)	Mean	88.5	27.0	0.653	0.692
		SD	21.8	13.7	0.085	0.018
60	WT (n=8)	Mean	130.4	15.6	0.489	0.688
		SD	15.9	3.7	0.063	0.009
	KO (n=8)	Mean	126.4	19.1	0.504	0.690
		SD	20.10	8.73	0.079	0.015
70	WT (n=8)	Mean	162.4	11.0	0.363	0.689
		SD	14.9	2.0	0.059	0.009
	KO (n=8)	Mean	161.1	14.1	0.368	0.691
		SD	19.2	2.9	0.075	0.015

WT = wild-type; KO = knock-out; EI = echo intensity; TAI = texture anisotropy index; GSI = gray-scale index; SD = standard deviation; CoV = coefficient of variation.